Can we filter non-stationary noise from geodetic data with fast spectral (FFT) techniques ?

Christopher Kotsakis
Department of Geomatics Engineering, University of Calgary
2500 University Drive NW, Calgary, Alberta, Canada T2N 1N4
Tel.: +1-403-2204703, Fax: +1-403-2841980, Email: ckotsaki@ucalgary.ca

Abstract

An important problem in the practical implementation of optimal spectral methods in gravity field modelling is the stationarity assumption for the input data noise and the underlying unknown signals. Such a restriction is required, according to the standard Wiener-Kolmogorov linear estimation theory for random fields, in order to obtain signal approximation algorithms of simple filtering (i.e. convolution) structure that can be evaluated very efficiently through fast Fourier transform numerical techniques. Often, the observation errors in the input data have significant spatial variations in their statistical behaviour, thus making the noise stationarity assumption unrealistic for many practical situations. Additionally, a stochastic interpretation of the true values of the various gravity field signals as random variables with similar statistical parameters is rather questionable, since they describe physical phenomena that are not random (probabilistic) and certainly do not have a uniform (stationary) behaviour over their domain. The aim of the paper is to present a spectral Wiener-type optimal noise filter that can be used in geodetic estimation problems regardless of the spatio-statistical properties of the underlying signals and the measurement errors. Some numerical examples have also been included to demonstrate the performance of the new filter under non-stationary uncorrelated noise at different sampling resolution levels, using a synthetic two-dimensional grid of noisy gravity anomaly data.

1. Introduction

The use of spectral methods in gravity field approximation problems has reached a considerable level of maturity over the past years, placing them among the standard tools of modern operational geodesy. Particularly the optimal combination and processing of regional data grids (e.g., gravity anomalies, altimetric data, digital elevation models, deflections of the vertical, etc.), for either land or marine geoid modelling, can be very efficiently implemented with frequency-domain techniques, resulting to what is commonly known in the geodetic literature as an input-output (I/O) linear estimation system. In SIDERIS [1996] a general description of such optimal spectral methods for solving physical geodesy estimation problems was given, which closely adheres to the mathematical formalism and terminology found in the textbooks by BENDAT AND PIERSOL [1986, 1993]; see also SCHWARZ ET AL. [1990]. The comparison of the I/O systems theory with other linear approximation techniques traditionally used in geodesy (i.e. least-squares collocation) was discussed in detail by SANSO AND SIDERIS [1997] within the unifying framework of the Wiener-Kolmogorov (W-K) optimal prediction theory for random fields. Many numerical studies in gravity field modelling have been performed over the last years using the versatility of optimal spectral methods, including: Wiener filtering of gravity anomaly data prior to gravimetric geoid computations [LI AND SIDERIS, 1994], optimal separation of the gravity anomaly signal from external noise (and other residual) effects for the identification of certain crustal geological features

[PAWLOWSKI AND HANSEN, 1990], optimal combination of shipborne gravity and altimetric data for marine geoid modelling [LI, 1996; TZIAVOS ET AL., 1996, 1998], simultaneous optimal noise filtering of airborne gravity vector data [WU AND SIDERIS, 1995], and optimal estimation of the anomalous potential from airborne gradiometry data [VASSILIOU, 1986], among numerous other publications.

A crucial point in the practical implementation of a frequency-domain I/O estimation system for geoid computations has always been the assumption that the measurement noise in the various data sets follows a stationary probabilistic model. Such a hypothesis, in conjunction with: (i) an additional stationarity assumption for the underlying (true) gravity field signals, (ii) a mean square error (MSE) optimal criterion, and (iii) the fact that the unknown fields involved in geodetic problems are related through convolution operators*, lead to simple signal estimation equations of filtering type which can be evaluated very efficiently using fast Fourier transform (FFT) numerical techniques. This provides a definite computational advantage over the equivalent space-domain algorithm of least-squares collocation, especially for large data grids with high sampling resolution. In the case of non-stationary noise and/or signals, on the other hand, the W-K optimal estimation theory can no longer be expressed in terms of straightforward linear filtering (i.e. convolution) operations, thus making the spectral algorithms of I/O systems theory quite complex and unsuitable for efficient evaluation via FFT routines; for more details, see SANSO AND SIDERIS [1997].

The goal of this paper is to assemble a convolution-type algorithmic procedure (suitable for FFT-based implementation) that can be used in geodetic estimation problems regardless of the statistical properties of the underlying signals and the data noise. The true fields will not even be associated with any probabilistic behaviour at all, but they will be treated as arbitrary deterministic signals. Our analysis is going to be restricted for the simple case where an unknown deterministic field is observed under the masking of non-stationary random observation errors, and the desired output corresponds to an improved ('de-noised') linear interpolating model of the noisy input data. This will provide us with a modified Wiener-type filter that can be used either as an independent practical tool for geodetic data pre-processing, or as an integral component of a more general I/O linear estimation system (e.g., for optimal spectral geoid determination from gravity anomaly grids). An important point in our approach is that the sampling resolution of the input data will be explicitly taken into account within the optimization procedure, resulting in a *resolution-dependent* noise filter. The interesting interplay that exists between measurement noise and data resolution in linear signal estimation will thus become more apparent, since in the relevant geodetic literature dealing with spectral gravity field approximation problems the roles of these two important factors have not been clearly distinguished. A numerical example, using a synthetic two-dimensional gravity anomaly grid, has also been included at the end of the paper to demonstrate the performance of our optimal noise filter under non-stationary additive noise at different sampling resolution levels.

---

* This is actually not a strict requirement in order to have estimation algorithms of convolution structure. However, it allows the efficient application of variance-covariance propagation in gravity field signals through simple filtering spectral relationships.

2. Notation and other preliminary issues

The main assumptions and the basic mathematical notation that will be used throughout the rest of this paper are presented in this section. We will follow a relatively simple approximation framework in a two-dimensional (2D) planar setting which, nevertheless, can fit nicely to many spatial geodetic estimation problems of local or regional scale. The unknown object of the estimation procedure will be modelled as a 2D deterministic signal $g(x,y)$ with compact spatial support over the real plane $\Re^2$. Its finite extent along the two orthogonal axes *x* and *y* is denoted by *X* and *Y*, respectively. No specific smoothing restrictions on the behaviour of the unknown field will be imposed, apart from the assumption that it posses a well-defined 2D Fourier transform, i.e.

$$G(\omega_x,\omega_y) = \int_{-\infty}^{+\infty}\int_{-\infty}^{+\infty} g(x,y)\, e^{-i(\omega_x x+\omega_y y)}\, dx\, dy \tag{1}$$

The two parameters ω_x and ω_y are the spatial circular frequencies along the *x* and *y* axes, respectively. A regular grid of true signal values will be denoted by $g(nh_x, mh_y)$, where the symbols h_x and h_y correspond to the orthogonal sampling intervals along the *x* and *y* directions. Without loss of generality, we can assume that the compact support of the unknown field is enclosed by the region $0 \le x \le X$ and $0 \le y \le Y$, and thus the integer sampling indices can practically be restricted within the finite range $0 \le n \le N-1$ and $0 \le m \le M-1$, where $X=(N-1)\,h_x$ and $Y=(M-1)\,h_y$. The 2D Fourier transform of such a noiseless signal grid will be denoted by $\overline{G}(\omega_x,\omega_y)$ and it is given by the summation formula [DUDGEON AND MERSEREAU, 1984]

$$\begin{aligned}
\overline{G}(\omega_x,\omega_y) &= \sum_{n=-\infty}^{+\infty}\sum_{m=-\infty}^{+\infty} g(nh_x, mh_y)\, e^{-i(nh_x\omega_x + mh_y\omega_y)} \\
&= \sum_{n=0}^{N-1}\sum_{m=0}^{M-1} g(nh_x, mh_y)\, e^{-i(nh_x\omega_x + mh_y\omega_y)} \\
&= \frac{1}{h_x h_y}\sum_{k=-\infty}^{+\infty}\sum_{l=-\infty}^{+\infty} G(\omega_x + \frac{2\pi k}{h_x}, \omega_y + \frac{2\pi l}{h_y})
\end{aligned} \tag{2}$$

where the last part in the above equation expresses the aliasing effect on the Fourier transform of the original continuous signal. The overbar symbol will generally be used to indicate a periodic function, and the lower case letters *n*, *m*, *k*, *l* are always reserved to denote integer numbers. The input data obtained from the unknown field is given in a discrete gridded form according to the linear observation equation

$$d(nh_x, mh_y) = g(nh_x, mh_y) + v(nh_x, mh_y) \tag{3}$$

where $v(nh_x, mh_y)$ is a 2D random noise sequence that is generally assumed non-stationary. The associated stochastic model used to describe the behaviour of the measurement noise, in terms of second-order moment information, is defined by the following equations:

$$E\left\{v(nh_x, mh_y)\right\} = 0 \tag{4a}$$

$$E\left\{v^2(nh_x, mh_y)\right\} = \sigma_v^2(nh_x, mh_y) = \sigma_v\left[(nh_x, mh_y)(nh_x, mh_y)\right] \tag{4b}$$

$$E\left\{v(nh_x, mh_y)\, v(kh_x, lh_y)\right\} = \sigma_v\left[(nh_x, mh_y)(kh_x, lh_y)\right] \tag{4c}$$

where E is the probabilistic expectation operator. The symbol $\sigma_v^2(\cdot)$ denotes the noise variance at a specific data point on the real plane, whereas $\sigma_v\left[(\cdot)(\cdot)\right]$ corresponds to the noise covariance (CV) between two data points. We will also use the symbol $\overline{V}(\omega_x, \omega_y)$ for the 2D Fourier transform of the random observation errors, which is defined as

$$\begin{aligned} \overline{V}(\omega_x,\omega_y) &= \sum_{n=-\infty}^{+\infty} \sum_{m=-\infty}^{+\infty} v(nh_x, mh_y)\, e^{-i(nh_x\omega_x + mh_y\omega_y)} \\ &= \sum_{n=0}^{N-1} \sum_{m=0}^{M-1} v(nh_x, mh_y)\, e^{-i(nh_x\omega_x + mh_y\omega_y)} \end{aligned} \tag{5}$$

Similarly, the 2D Fourier transform of the gridded data is given by the equation

$$\begin{aligned} \overline{D}(\omega_x,\omega_y) &= \sum_{n=-\infty}^{+\infty} \sum_{m=-\infty}^{+\infty} d(nh_x, mh_y)\, e^{-i(nh_x\omega_x + mh_y\omega_y)} \\ &= \sum_{n=0}^{N-1} \sum_{m=0}^{M-1} d(nh_x, mh_y)\, e^{-i(nh_x\omega_x + mh_y\omega_y)} \\ &= \overline{G}(\omega_x,\omega_y) + \overline{V}(\omega_x,\omega_y) \end{aligned} \tag{6}$$

Note that the noise signal is zero outside the input data grid (*NM* points), since the unknown field $g(x, y)$ has been assumed to have finite spatial support and thus no measurements are performed outside this region.

3. Problem formulation

Two basic properties will be imposed a-priori in the estimation algorithm, namely linearity and translation-invariance. The reason for introducing the second property is to obtain a signal estimate $\hat{g}(x,y)$ that is independent of the reference system used to describe the position of the data points. Stated in a simplified way, if we change the origin of the 2D reference system xy on the real plane by arbitrary translations (without 'moving' the unknown field or the associated data grid), we want the new signal approximation to be just a translated version of the initial estimate that was obtained in the original reference system.

The justification of such a modelling choice relies basically on simple logic and mathematical intuition, and it is not affected by the spatio-statistical properties of the true signal and noise involved in the specific approximation problem. If one chooses to follow a non translation-invariant methodology (e.g., Tikhonov regularization in a Hilbert space with a non-homogeneous reproducing kernel), he should at least be able to explain physically the dependence of the output signal estimate on the origin of the coordinate system used to reference the unknown field and its discrete input data. Note that the translation-invariance condition has often been applied in the theoretical formulation of optimal estimation methods using errorless discrete data [SANSO, 1980; KOTSAKIS, 2000a], although its justification is not altered by the presence of noise in the input observations.

Based on the two assumptions of linearity and translation-invariance, the signal estimation formula will have the general convolution-type expression

$$\hat{g}(x,y) = \sum_{n=0}^{N-1} \sum_{m=0}^{M-1} d(nh_x, mh_y)\, \xi_h(x - nh_x, y - mh_y) \tag{7}$$

where $\xi_h(x,y)$ is a 2D filtering kernel that needs to be determined in some optimal sense. The subscript h is used to indicate that the estimation kernel will generally depend on the data resolution levels, h_x and h_y. The above equation can be illustrated through the linear I/O system shown in Figure 1.

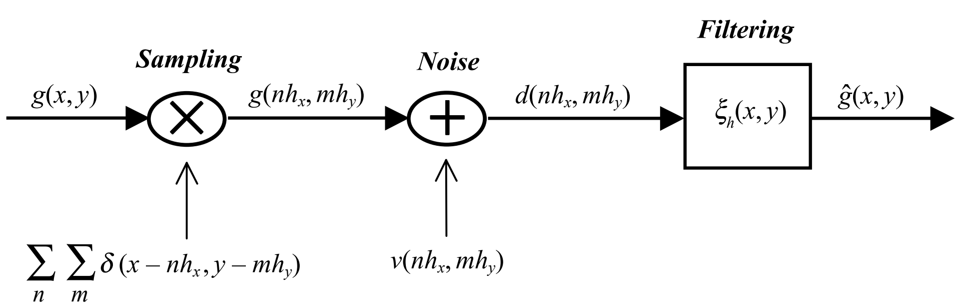

Figure 1. Linear and translation-invariant signal estimation from discrete noisy data.

4. Minimization of the noise-dependent signal estimation error

The output signal error produced by the filtering formula in Eq. (7) can generally be decomposed into two components

$$\begin{aligned} e(x,y) &= g(x,y) - \hat{g}(x,y) \\ &= e_h(x,y) + e_v(x,y) \end{aligned} \tag{8}$$

where $e_h(x,y)$ is the part of the total estimation error caused from the use of discrete data with finite sampling resolution (aliasing error), and $e_v(x,y)$ is the additional part due to the noise presence in the signal samples. In the absence of any noise from the discrete input data, the best we could do is to obtain just an *interpolated model* $\breve{g}(x,y)$ for the unknown field that will depend on the true signal values at the given spatial resolution. It will be assumed that such a noiseless signal model is given in terms of a linear and translation-invariant formula, as follows:

$$\breve{g}(x,y) = \sum_{n=0}^{N-1} \sum_{m=0}^{M-1} g(nh_x, mh_y)\, \varphi_h(x-nh_x,\, y-mh_y) \tag{9}$$

where $\varphi_h(x,y)$ is some basic interpolating kernel that generally depends on the sampling intervals h_x and h_y. The noise-dependent estimation error will be measured with respect to such a linear interpolating model for the unknown field, i.e.

$$e_v(x,y) = \breve{g}(x,y) - \hat{g}(x,y) \tag{10a}$$

whereas the (pure) aliasing error is

$$e_h(x,y) = g(x,y) - \breve{g}(x,y) \tag{10b}$$

The specific form of the modelling kernel in Eq. (9) is irrelevant for the purpose of this paper. A very popular choice that covers many different linear interpolating schemes, including band-limited (Shannon) interpolation, spline-based interpolation and also more general wavelet approximation models, is based on the use of certain scaling functions $\varphi(x,y)$ which adapt to the data grid resolution through a dilation operation [UNSER, 2000], i.e.

$$\varphi_h(x,y) = \varphi\left(\frac{x}{h_x}, \frac{y}{h_y}\right) \tag{11}$$

The optimal determination of such interpolating scaling kernels, and their connection with the statistical collocation and wavelet theory, were discussed in KOTSAKIS [2000a, b]. The behaviour of the aliasing error term $e_h(x,y)$ for different choices of the scaling function $\varphi(x,y)$ and the data resolution level was also studied in KOTSAKIS [2000b] and KOTSAKIS AND SIDERIS [2000]. For the purpose of this paper, it is sufficient to consider $\varphi_h(x,y)$ in Eq. (9) as an arbitrarily chosen interpolating kernel with a well-defined Fourier transform $\Phi_h(\omega_x,\omega_y)$, which is used to obtain a continuous signal approximation in the absence of any noise from the discrete input data. In addition, it can be assumed that $\varphi_h(x,y)$ is such that: (i) the signal expansion in Eq. (9) is always stable, and (ii) the aliasing error component $e_h(x,y)$ vanishes as the data resolution increases; for more details, see KOTSAKIS [2000b] and BLU AND UNSER [1999].

The filtering kernel in Eq. (7) will be determined by minimizing the noise-dependent part of the total signal error. In this way, the signal estimation problem is essentially reduced to a problem of finding an optimal modification for the interpolating kernel $\varphi_h(x,y)$ that minimizes the effect of the propagated data noise in the final output field $\hat{g}(x,y)$. The optimization procedure will be carried out in the frequency domain using the familiar MSE criterion

$$P_{e_v}(\omega_x,\omega_y) = E\left\{ \left|E_v(\omega_x,\omega_y)\right|^2 \right\} = \text{minimum} \tag{12}$$

where $E_v(\omega_x,\omega_y)$ is the 2D Fourier transform of $e_v(x,y)$, and $P_{e_v}(\omega_x,\omega_y)$ is the (noise-dependent) mean error power spectrum of the estimated output signal. From Eqs. (7), (9) and (10a), we have that

$$\begin{aligned} E_v(\omega_x,\omega_y) = {} & \Phi_h(\omega_x,\omega_y) \sum_{n=0}^{N-1} \sum_{m=0}^{M-1} g(nh_x, mh_y)\, e^{-i(nh_x\omega_x + mh_y\omega_y)} \\ & - \Xi_h(\omega_x,\omega_y) \sum_{n=0}^{N-1} \sum_{m=0}^{M-1} d(nh_x, mh_y)\, e^{-i(nh_x\omega_x + mh_y\omega_y)} \end{aligned} \tag{13a}$$

where $\Xi_h(\omega_x,\omega_y)$ is the Fourier transform of the unknown filtering kernel $\xi_h(x,y)$. Using the shorthand notation according to Eqs. (2) and (6), the last equation takes the form

$$E_v(\omega_x,\omega_y) = \Phi_h(\omega_x,\omega_y)\,\overline{G}(\omega_x,\omega_y) - \Xi_h(\omega_x,\omega_y)\,\overline{G}(\omega_x,\omega_y) - \Xi_h(\omega_x,\omega_y)\,\overline{V}(\omega_x,\omega_y) \tag{13b}$$

By multiplying the above expression with its complex conjugate and taking the expected value, we can finally obtain the (noise-dependent) mean error power spectrum of the output signal, as follows:

$$
\begin{aligned}
P_{e_v}(\omega_x,\omega_y) \;=\; & \Phi_h(\omega_x,\omega_y)\,\Phi_h^*(\omega_x,\omega_y)\left|\overline{G}(\omega_x,\omega_y)\right|^2 \\
& - \Phi_h(\omega_x,\omega_y)\,\Xi_h^*(\omega_x,\omega_y)\left|\overline{G}(\omega_x,\omega_y)\right|^2 \\
& - \Phi_h^*(\omega_x,\omega_y)\,\Xi_h(\omega_x,\omega_y)\left|\overline{G}(\omega_x,\omega_y)\right|^2 \\
& + \Xi_h(\omega_x,\omega_y)\,\Xi_h^*(\omega_x,\omega_y)\left|\overline{G}(\omega_x,\omega_y)\right|^2 \\
& + \Xi_h(\omega_x,\omega_y)\,\Xi_h^*(\omega_x,\omega_y)\,\overline{P}_v(\omega_x,\omega_y)
\end{aligned}
\tag{14}
$$

where * denotes complex conjugation, and the auxiliary term $\overline{P}_v(\omega_x,\omega_y)$ corresponds to the noise 'power spectral density (PSD)' function

$$
\overline{P}_v(\omega_x,\omega_y) \;=\; E\left\{\overline{V}(\omega_x,\omega_y)\,\overline{V}^*(\omega_x,\omega_y)\right\} = E\left\{\left|\overline{V}(\omega_x,\omega_y)\right|^2\right\}
\tag{15}
$$

For the derivation of the result in Eq. (14) we have used the fact that $E\left\{\overline{V}(\omega_x,\omega_y)\right\}=0,$ in accordance with the zero-mean stochastic model introduced for the data noise in Eq. (4a). It can easily be verified that the optimal estimation filter will be finally given by the following formula:

$$
\begin{aligned}
\Xi_h(\omega_x,\omega_y) \;&=\; \frac{\left|\overline{G}(\omega_x,\omega_y)\right|^2}{\left|\overline{G}(\omega_x,\omega_y)\right|^2 + \overline{P}_v(\omega_x,\omega_y)}\;\Phi_h(\omega_x,\omega_y) \\
&= \overline{W}(\omega_x,\omega_y)\;\Phi_h(\omega_x,\omega_y)
\end{aligned}
\tag{16}
$$

5. The separable structure of the optimal estimation filter

The final result in Eq. (16) indicates that the optimal estimation procedure can be decomposed into two individual steps which are connected in a linear cascading manner. The first step, expressed by the periodic filter component $\overline{W}(\omega_x,\omega_y)$, has the role of 'de-noising' the discrete input data using information about the average behaviour of the input noise and the unknown field at the given resolution level. The second filter component $\Phi_h(\omega_x,\omega_y)$, on the other hand, is solely used to obtain a continuous representation for the output signal based on an a-priori selected interpolating/modelling kernel $\varphi_h(x,y)$. These two basic steps of the optimal estimation procedure are illustrated in the linear I/O system of Figure 2.

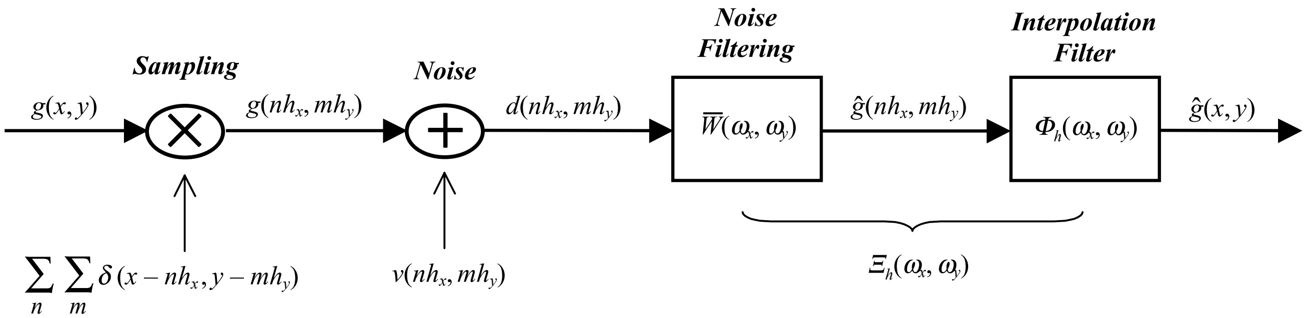

Figure 2. The cascading structure of the optimal linear estimation filter.

As it can be seen from the above figure, it is not really necessary to 'modify' the interpolating kernel $\varphi_h(x,y)$ of the reference signal model in Eq. (9) when dealing with noisy input data. The optimization of the noise-dependent output error adds only an intermediate periodic filter that is applied to the original data grid, and it produces a new estimated signal sequence $\hat{g}(nh_x, mh_y)$ from which the effect of the random observational errors has been minimized in a certain translation-invariant MSE sense. We can then use this new sequence as input to the basic interpolating model of Eq. (9), in order to get a continuous (also linear and translation-invariant) approximation of the unknown field at the given resolution level. It should be noted that the interpolation filter in Figure 2 can be also optimized by following a separate MSE approach that takes into account only the noise-free error component $e_h(x,y)$, as it is described in KOTSAKIS [2000a, b].

The structure of the optimal noise filter in Eq. (16) is very similar to the classic Wiener estimation filter, since they are both defined in terms of a signal-to-noise ratio (SNR) expression. However, there do exist conceptual differences between the two filtering schemes because in our formulation: (i) the unknown field has been modelled as a deterministic (instead of stochastic) signal, and (ii) the additive data noise has not been restricted to being stationary. Therefore, it is important to clarify what is the exact meaning of the two frequency-domain terms that appear in the SNR expression of our noise filter $\overline{W}(\omega_x,\omega_y)$. From Eq. (16), we have that

$$\begin{aligned}
\overline{W}(\omega_x,\omega_y) &= \frac{\left|\overline{G}(\omega_x,\omega_y)\right|^2}{\left|\overline{G}(\omega_x,\omega_y)\right|^2 + \overline{P}_v(\omega_x,\omega_y)} \\
&= \frac{\frac{1}{NM}\left|\overline{G}(\omega_x,\omega_y)\right|^2}{\frac{1}{NM}\left|\overline{G}(\omega_x,\omega_y)\right|^2 + \frac{1}{NM}\,\overline{P}_v(\omega_x,\omega_y)} \\
&= \frac{\overline{A}(\omega_x,\omega_y)}{\overline{A}(\omega_x,\omega_y) + \overline{B}(\omega_x,\omega_y)}
\end{aligned} \tag{17}$$

where NM is the total number of points in the input data grid. The two auxiliary functions, $\overline{A}(\omega_x,\omega_y)$ and $\overline{B}(\omega_x,\omega_y)$, in the last equation correspond to the Fourier transforms of two associated sequences which have the CV-like expressions

$$a(nh_x, mh_y) = \frac{1}{NM} \sum_{k=0}^{N-1} \sum_{l=0}^{M-1} g\big(kh_x, lh_y\big)\, g\big((k+n)h_x, (l+m)h_y\big) \tag{18a}$$

and

$$b(nh_x, mh_y) = \frac{1}{NM} \sum_{k=0}^{N-1} \sum_{l=0}^{M-1} \sigma_v\Big[\big(kh_x, lh_y\big)\,\big((k+n)h_x, (l+m)h_y\big)\Big] \tag{18b}$$

respectively. The first sequence in Eq. (18a) can easily be identified as the discrete spatial CV function of the true deterministic signal at the given data resolution level, and thus the term $\overline{A}(\omega_x,\omega_y)$ in Eq. (17) corresponds to the power spectrum of the true signal values $g(nh_x, mh_y)$. Note that $a(nh_x, mh_y)$ contains less spatio-statistical information than the continuous signal CV function, since it takes into account only the discrete values of the unknown field at a certain resolution.

The second sequence in Eq. (18b), on the other hand, does not exactly correspond to the discrete noise CV function and, as a result, the frequency-domain quantity $\overline{B}(\omega_x,\omega_y)$ in Eq. (17) should not generally be viewed as the PSD of the data noise. Such an interpretation is possible only in the special case where the input noise is stationary. Indeed, in such situation the noise covariance σ_v between two arbitrary data points with coordinates $\big(kh_x, lh_y\big)$ and $\big((k+n)h_x, (l+m)h_y\big)$ becomes a function of their coordinate differences only, which are obviously equal to (nh_x, mh_y). Therefore, σ_v can be taken outside of the summation operator in Eq. (18b), leaving the summation result equal to NM.

In the more general case of non-stationary noise, the sequence $b(nh_x, mh_y)$ can be interpreted as a 'mean' CV function of the random observation errors. Its value at the origin gives an average indication of the noise level at every point of the input data grid, i.e.

$$\begin{aligned} b(0,0) &= \frac{1}{NM} \sum_{k=0}^{N-1} \sum_{l=0}^{M-1} \sigma_v\big[(kh_x, lh_y)\,(kh_x, lh_y)\big] \\ &= \frac{1}{NM} \sum_{k=0}^{N-1} \sum_{l=0}^{M-1} \sigma_v^2(kh_x, lh_y) \end{aligned} \tag{19}$$

whereas its values $b(nh_x, mh_y)$ at other points correspond to 'averages' of the noise covariance over pairs of data points with coordinate differences (nh_x, mh_y). Note that both sequences in Eqs. (18a) and (18b) are always symmetric, and they take zero values outside the range $-(N-1) \le n \le (N-1)$ and $-(M-1) \le m \le (M-1)$ due to the finite spatial support of the input signal $g(x,y)$. Also, in practice the computation of the optimal noise filter $\overline{W}(\omega_x,\omega_y)$ can take place only at a discrete finite set of frequency values by using the FFTs of the two sequences given in Eqs. (18a) and (18b).

6. Additional remarks

A key point in our estimation procedure was the decomposition of the output signal error into an aliasing part $e_h(x,y)$ and a noise-dependent part $e_v(x,y)$. The advantage of such a partition is that it allows us to study and optimize individually the effects of the finite data resolution and the input noise on the final signal estimate $\hat{g}(x,y)$, using appropriate error measures and criteria for each case. It should be kept in mind that the error component $e_h(x,y)$ is a purely deterministic signal whose average behaviour (at a given data resolution level) can only be modelled in a spatio-statistical sense through the concept of different 'sampling phases' [KOTSAKIS, 2000b; KOTSAKIS AND SIDERIS, 2000], whereas the noise-dependent error term $e_v(x,y)$ is a random signal whose average behaviour is described probabilistically with the notion of different 'experiment repetitions' (expectation operator E).

An important aspect for geodetic applications is also the numerical evaluation of the optimal noise filter $\overline{W}(\omega_x,\omega_y)$ given in Eq. (17). Although the noise PSD-like term $\overline{P}_v(\omega_x,\omega_y)$ can always be determined from the known noise variances and covariances using FFT techniques, the signal 'PSD' term $\left|\overline{G}(\omega_x,\omega_y)\right|^2$ is generally unknown in practice. In order to overcome this difficulty, we can use the power spectrum of the available noisy data $d(nh_x,nh_y)$ to infer the behaviour of the signal 'PSD' function that is needed in the computation of the SNR-type noise filter. From Eq. (6), we can express the power spectrum of the data values as follows:

$$\begin{aligned}\left|\overline{D}(\omega_x,\omega_y)\right|^2 &= \left(\overline{G}(\omega_x,\omega_y)+\overline{V}(\omega_x,\omega_y)\right)\left(\overline{G}(\omega_x,\omega_y)+\overline{V}(\omega_x,\omega_y)\right)^* \\ &= \left|\overline{G}(\omega_x,\omega_y)\right|^2+\overline{G}(\omega_x,\omega_y)\,\overline{V}^*(\omega_x,\omega_y)+\overline{G}^*(\omega_x,\omega_y)\,\overline{V}(\omega_x,\omega_y)+\left|\overline{V}(\omega_x,\omega_y)\right|^2\end{aligned} \tag{20a}$$

and by applying the expectation operator to the above formula, we finally get

$$\begin{aligned}E\left\{\left|\overline{D}(\omega_x,\omega_y)\right|^2\right\} &= \left|\overline{G}(\omega_x,\omega_y)\right|^2 + E\left\{\left|\overline{V}(\omega_x,\omega_y)\right|^2\right\} \\ &= \left|\overline{G}(\omega_x,\omega_y)\right|^2 + \overline{P}_v(\omega_x,\omega_y)\end{aligned} \tag{20b}$$

The unknown signal term $\left|\overline{G}(\omega_x,\omega_y)\right|^2$ can now be determined empirically through Eq. (20b) by taking the available realization $\left|\overline{D}(\omega_x,\omega_y)\right|^2$ of the data power spectrum as an estimate of its expected value.

Finally, let us briefly comment on the effect of the data sampling resolution on the noise-dependent output signal error. The use of the optimal estimation filter according to Eq. (16) leads to the following expression for the mean power spectrum of the signal error $e_v(x,y)$:

$$
\begin{aligned}
P_{e_v}(\omega_x,\omega_y) &= \frac{\left|\overline{G}(\omega_x,\omega_y)\right|^2}{\left|\overline{G}(\omega_x,\omega_y)\right|^2 + \overline{P}_v(\omega_x,\omega_y)} \; \overline{P}_v(\omega_x,\omega_y) \; \left|\Phi_h(\omega_x,\omega_y)\right|^2 \\
&= \overline{W}(\omega_x,\omega_y) \; \overline{P}_v(\omega_x,\omega_y) \; \left|\Phi_h(\omega_x,\omega_y)\right|^2
\end{aligned}
\tag{21}
$$

The above formula can easily be derived by substituting the optimal result of Eq. (16) into Eq. (14). Note that the noise-dependent error component $e_v(x,y)$ is not completely unaffected by the input data resolution, but it actually depends on it. In order to see more clearly this important implicit relationship, let us adopt a rather general model for the reference interpolating kernel $\varphi_h(x,y)$. In particular, we shall consider the case where the noiseless signal interpolating model has the scaling form

$$
\varphi_h(x,y) = \varphi(\frac{x}{h_x},\frac{y}{h_y}) \tag{22}
$$

where $\varphi(x,y)$ is some basic scaling kernel (e.g., *sinc* function in the case of band-limited approximation). Taking into account the fundamental scaling property of the 2D Fourier transform [DUDGEON AND MERSEREAU, 1984], the frequency-domain expression in Eq. (21) can now be written as

$$
P_{e_v}(\omega_x,\omega_y) = (h_x\, h_y)^2\, \overline{W}(\omega_x,\omega_y)\, \overline{P}_v(\omega_x,\omega_y) \left|\Phi(h_x\omega_x, h_y\omega_y)\right|^2 \tag{23}
$$

where $\Phi(\omega_x,\omega_y)$ is the Fourier transform of the scaling function $\varphi(x,y)$. Avoiding further mathematical details, it can be seen from the last equation that the noise-dependent estimation error will decrease as the resolution level of the input data increases (i.e. smaller sampling intervals h_x and h_y). Such a result is not surprising and it just confirms the (well-known from signal analysis theory) fact that oversampling leads to noise reduction in the final signal estimate (see, e.g., CVETKOVIĆ AND VETTERLI, 1998). An additional indication of this interesting behaviour is also given in the next section using simulated numerical data.

7. Numerical simulations

In this section we will test numerically the noise filtering component of the optimal estimation kernel that was derived in Sect. 4; see Eq. (16). Hence, we shall not implement the whole I/O linear estimation system shown in Figure 2, but we will restrict our attention only on its first 'de-noising' part that transforms the original input data into an improved filtered signal sequence. The second interpolatory step through the use of a reference modelling kernel $\varphi_h(x,y)$ will be omitted.

A two-dimensional deterministic signal $g(x,y)$, assumed to represent some local gravity anomaly field, was initially synthesized using a truncated Fourier series expansion with a record length of 200 × 200 km (see Figures 3 and 4). The continuous signal was sampled at various uniform resolution levels $h_x \times h_y$ to obtain noiseless gridded values $g(nh_x, mh_y)$. Four different sampling resolutions were selected, namely 0.5 × 0.5, 1.0 × 1.0, 2.5 × 2.5 and 5.0 × 5.0 km. The sample statistics of the true signal values are given in Table 1. All the signal grids at each resolution level were partitioned into four equal blocks-quadrants, labeled as northwest (NW), northeast (NE), southwest (SW) and southeast (SE). The simulated data noise, which is going to be added to the true signal values, will have a different stochastic behaviour in each of the four grid quadrants.

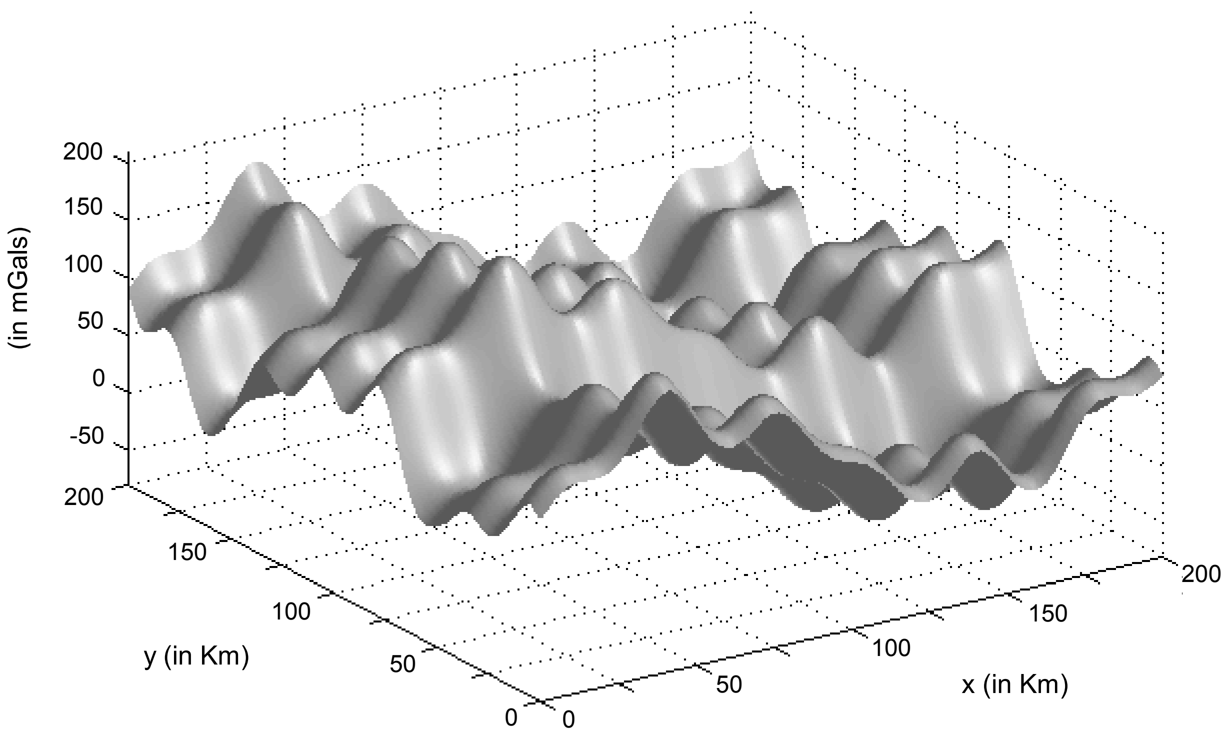

Figure 3. The original (simulated) gravity anomaly field shown as a 3D surface plot.

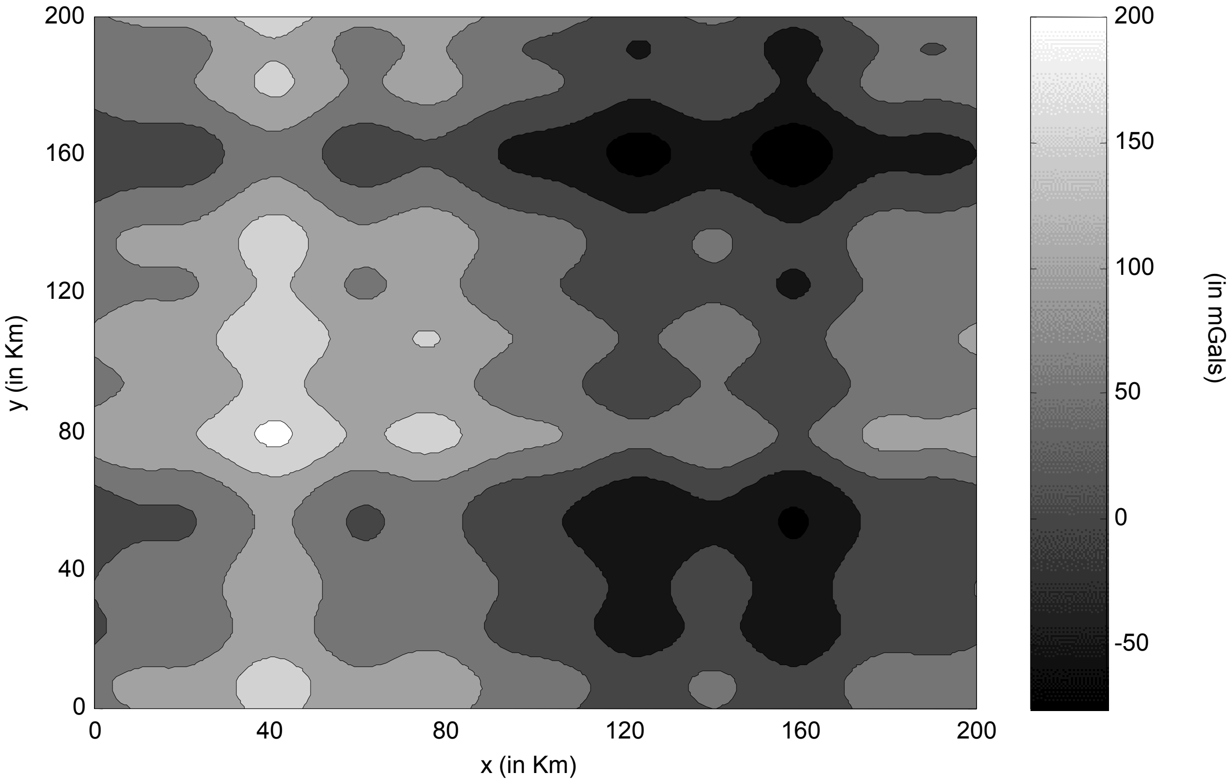

Figure 4. The simulated gravity anomaly field shown as a black and white image plot.

Table 1. Statistics of the true signal values at various sampling resolution levels (in mGals).

Data resolution (in Km)	**0.5 × 0.5**	**1.0 × 1.0**	**2.5 × 2.5**	**5.0 × 5.0**
Max	206.64	206.55	206.30	206.30
Mean	62.33	62.39	62.56	62.84
Min	-75.49	-75.36	-75.02	-74.50
Std	52.12	52.07	51.92	51.67
RMS	81.26	81.26	81.29	81.36

A zero-mean noise sequence $v(nh_x, mh_y)$ was added to the samples of the true signal in order to create the input data at every resolution level, according to the form $d(nh_x, mh_y) = g(nh_x, mh_y) + v(nh_x, mh_y)$. The noise values originated from a non-stationary and uncorrelated Gaussian stochastic process, using the routines for random number generation of the MATLAB™ software package. Note that the noise values were generated separately at each resolution, instead of simply decimating the noise sequence with the smaller sampling interval. The noise variance $\sigma_v^2(nh_x, mh_y)$ was constant within each quadrant (NW, NE, SW and SE) of the data grids, with its values set to 144 mGals^2, 9 mGals^2, 144 mGals^2 and 49 mGals^2, respectively (see Figure 5). The sample statistics of the total noise sequence $v(nh_x, mh_y)$ at every resolution level are given in Table 2, whereas the individual sample statistics of the noise values in the four different parts of the data grids are shown in Tables 3a and 3b.

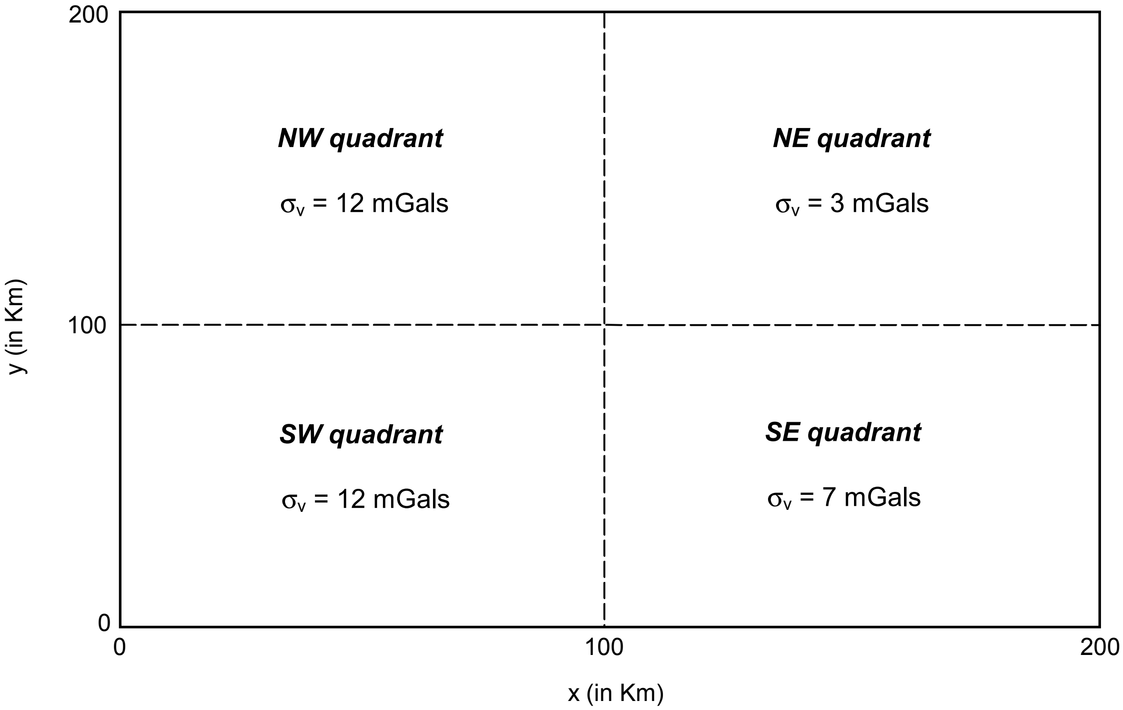

Figure 5. Partition of the input data grid into four equal quadrants. The standard deviation of the uncorrelated random noise that is added to the true signal samples varies spatially according to the simulating values shown in the figure.

Table 2. Statistics of the total additive noise at various sampling resolution levels (in mGals).

Data resolution (in Km)	**0.5 × 0.5**	**1.0 × 1.0**	**2.5 × 2.5**	**5.0 × 5.0**
Max	55.64	53.15	43.24	35.46
Mean	0.00	-0.01	0.05	-0.10
Min	-52.61	-52.71	-41.22	-38.84
Std	9.32	9.37	9.42	9.12
RMS	9.32	9.37	9.42	9.12

Table 3a. Statistics of the additive noise at different sampling resolutions in the four quadrants of the data grids (in mGals).

Data resolution (in Km)	**0.5 × 0.5**				**1.0 × 1.0**			
Grid quadrants	NW	SW	NE	SE	NW	SW	NE	SE
Max	49.61	55.64	12.47	27.37	53.15	43.04	11.45	25.88
Mean	-0.04	0.02	0.02	-0.01	0.03	0.01	0.02	-0.08
Min	-52.61	-46.34	-12.14	-27.14	-52.71	-47.87	-10.24	-28.58
Std	11.99	12.05	3.00	6.98	12.07	12.08	2.95	7.01
RMS	11.99	12.05	3.00	6.98	12.07	12.08	2.95	7.01

Table 3b. Statistics of the additive noise at different sampling resolution in the four quadrants of the data grids (in mGals).

Data resolution (in Km)	**2.5 × 2.5**				**5.0 × 5.0**			
Grid quadrants	NW	SW	NE	SE	NW	SW	NE	SE
Max	41.39	43.24	10.97	23.92	35.46	32.49	9.57	18.04
Mean	0.45	-0.24	0.10	-0.10	-0.92	0.11	0.29	0.10
Min	-40.49	-41.22	-11.15	-22.53	-34.00	-38.84	-9.81	-19.02
Std	11.94	12.19	3.07	7.12	11.86	11.36	3.07	6.84
RMS	11.95	12.20	3.07	7.12	11.90	11.36	3.08	6.84

The optimal noise filter $\overline{W}(\omega_x,\omega_y)$ was computed through an FFT algorithm at each resolution level $h_x \times h_y$, according to the SNR expression given in Eq. (17). It was then multiplied by the FFT of the noisy gridded data $d(nh_x,mh_y)$, and the result was finally transformed back to the space domain as an estimated ('de-noised') signal sequence $\hat{g}(nh_x,mh_y)$. The original noisy data grids are plotted in Figure 6 for some selective sampling resolution levels, whereas the corresponding filtered signal values are shown in Figure 7. The differences between the true signal samples and the estimated signal values are also shown in Figure 8, and their statistics are given in Table 4 below.

It is interesting to observe that the output estimation error of the filtered signal values $\hat{g}(nh_x,mh_y)$ is decreasing, as the data sampling intervals h_x, h_y become smaller. This is evident from the comparison of the three graphs shown in Figure 8, as well as from the error RMS values given in Table 4, and it confirms our earlier theoretical remark at the end of Sect. 6. Note also that the parts of the input data grid with the highest noise level (NW and SW quadrants) show larger estimation errors after the data filtering than the other two grid quadrants, as it should be intuitively expected (see also the values given in Tables 5a and 5b).

Table 4. Statistics of the differences between the true and the filtered signal values at various sampling resolution levels (in mGals).

Data resolution (in Km)	**0.5 × 0.5**	**1.0 × 1.0**	**2.5 × 2.5**	**5.0 × 5.0**
Max	3.09	3.51	5.53	6.26
Mean	0.00	0.01	-0.05	0.10
Min	-3.25	-4.00	-4.86	-8.01
Std	0.66	0.91	1.43	2.26
RMS	0.66	0.91	1.43	2.26

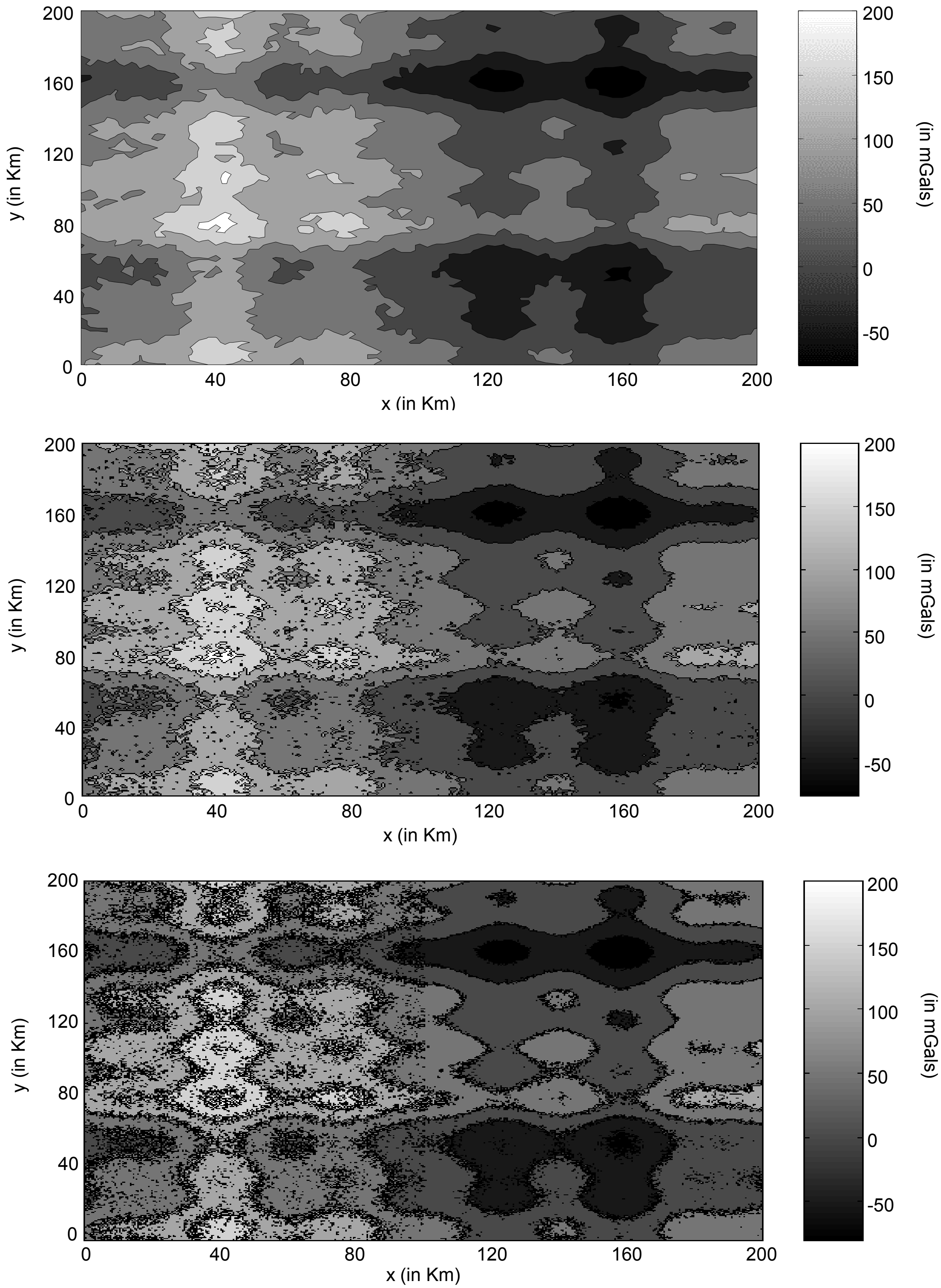

Figure 6. Noisy gravity anomaly values at various data resolution levels. The uniform gridding sampling intervals are 2.5×2.5 km (*top*), 1.0×1.0 km (*middle*) and 0.5×0.5 km (*bottom*).

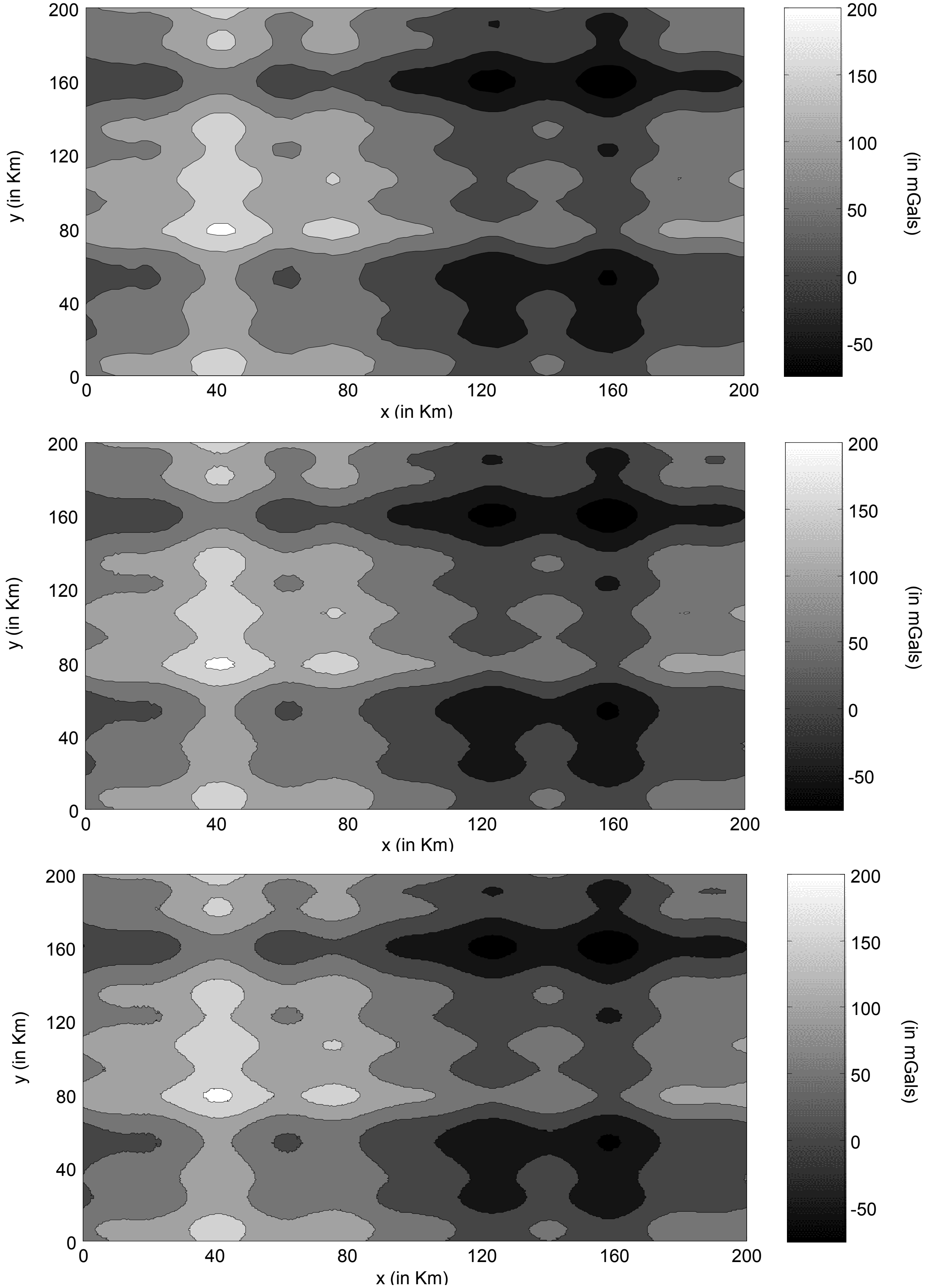

Figure 7. Estimated ('de-noised') gravity anomaly values at various data resolution levels. The uniform gridding sampling intervals are 2.5 × 2.5 km (*top*), 1.0 × 1.0 km (*middle*) and 0.5 × 0.5 km (*bottom*).

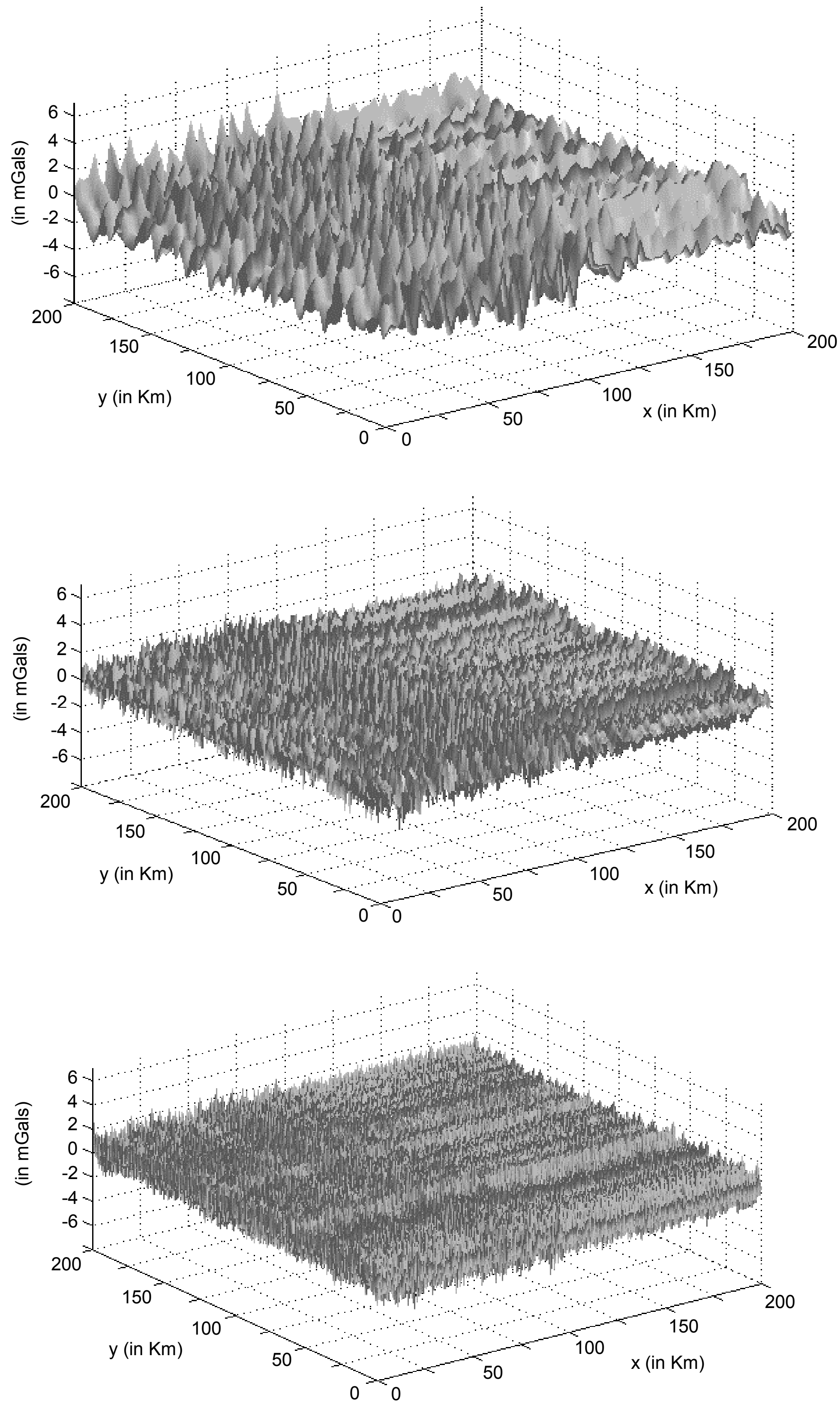

Figure 8. Differences between the true and the estimated (filtered) gravity anomaly values, at various data resolution levels. The uniform gridding sampling intervals are 2.5×2.5 km (*top*), 1.0×1.0 km (*middle*) and 0.5×0.5 km (*bottom*).

Table 5a. Statistics of the differences between the true and the filtered signal values at various sampling resolution levels in the four quadrants of the data grids (in mGals).

Data resolution (in Km)	**0.5 × 0.5**				**1.0 × 1.0**			
Grid quadrants	NW	SW	NE	SE	NW	SW	NE	SE
Max	2.75	3.09	1.97	2.30	3.51	3.38	2.63	2.50
Mean	0.02	0.00	0.00	-0.02	-0.05	0.01	0.00	0.06
Min	-2.89	-3.25	-2.08	-2.44	-3.59	-4.00	-2.35	-2.75
Std	0.72	0.78	0.52	0.60	1.06	1.04	0.76	0.74
RMS	0.72	0.78	0.52	0.60	1.06	1.04	0.76	0.74

Table 5b. Statistics of the differences between the true and the filtered signal values at various sampling resolution levels in the four quadrants of the data grids (in mGals).

Data resolution (in Km)	**2.5 × 2.5**				**5.0 × 5.0**			
Grid quadrants	NW	SW	NE	SE	NW	SW	NE	SE
Max	4.27	5.53	3.17	4.43	5.40	6.26	3.83	4.69
Mean	-0.33	0.12	-0.23	0.23	0.62	0.18	0.03	-0.41
Min	-4.86	-4.62	-2.93	-2.70	-8.01	-7.36	-5.30	-4.65
Std	1.57	1.71	1.02	1.22	2.47	2.60	1.76	1.93
RMS	1.60	1.71	1.04	1.24	2.55	2.61	1.76	1.97

8. Conclusions

A modification of the classic Wiener filtering method has been presented, which allows us to work with deterministic (instead of stochastic) signals that are masked by additive non-stationary noise at different sampling resolution levels. This provides a very useful estimation tool for many geodetic problems related to optimal spectral gravity field modelling. It has been shown that non-stationary noise filtering of geodetic data using fast spectral (i.e. FFT) techniques is possible, if we are willing to incorporate a simple translation-invariance condition into our signal approximation framework. Note that the traditional W-K linear prediction theory cannot lead to filtering (convolution) operations when the data noise is non-stationary. In such cases the estimation algorithm is reduced to a Fredholm equation of the first kind (Wiener-Hopf equation), whose solution determines the best linear (but ***not*** translation-invariant) signal estimate in a probabilistic MSE sense. In our approach, on the other hand, the a-priori imposed condition of translation-invariance allows us to treat both stationary and non-stationary noise cases within a unified linear filtering setting, which can be very efficiently implemented in practice via FFT numerical techniques.

Many important problems related to the work presented herein remain and require further research. Future work should include the extension of the planar spectral filtering algorithms for non-Euclidean domains of interest in geodesy, such as the sphere or the ellipsoid. Additional modifications are also needed in order to handle signal estimation applications that involve more than one type of input data (multiple-input/single-output systems), and not just the single-input/single-output case that was studied here. Nevertheless, the presented methodology can be proven a useful tool in many existing geodetic problems of regional or local scale, such as the optimal spectral geoid determination from noisy gridded gravity data or the FFT computation of various terrain-dependent gravity field quantities (e.g., indirect effect, terrain correction, isostatic potential, etc.) from noisy digital elevation models.

References

BENDAT, J.S. AND PIERSOL, A.G. (1986): *Random data: analysis and measurement procedures*. 2nd edition. John Wiley, New York.

BENDAT, J.S. AND PIERSOL, A.G. (1993): *Engineering applications of correlation and spectral analysis*. John Wiley, New York.

BLU, T. AND UNSER, M. (1999): Quantitative Fourier analysis of approximation techniques: Part I (Interpolators and projectors) and Part II (Wavelets). *IEEE Transactions on Signal Processing*, **47**(10), pp. 2783-2806.

CVETKOVIĆ, Z. AND VETTERLI, M. (1998): Overcomplete expansions and robustness. In: Zeevi, Y. and Coifman, R. (eds.) “Signal and image representation in combined spaces”, Academic Press, New York, pp. 301-338.

DUDGEON, D.E. AND MERSEREAU, R.M. (1984): *Multidimensional digital signal processing*. Prentice-Hall, Englewood Cliffs.

KOTSAKIS, C. (2000a): The multiresolution character of collocation. *Journal of Geodesy*, **74**(3-4), pp. 275-290.

KOTSAKIS, C. (2000b): Multiresolution aspects of linear approximation methods in Hilbert spaces using gridded data. *UCGE Report No. 20138*, Dept. of Geomatics Engineering, University of Calgary, Calgary, Alberta.

KOTSAKIS, C. AND SIDERIS, M.G. (2000): Aliasing error modelling in single-input single-output linear estimation systems. Paper presented at the *IAG international symposium on Gravity, Geoid and Geodynamics*, Banff, Alberta, July 31- August 4.

LI, J. (1996): Detailed marine gravity field determination by combination of heterogeneous data. *UCGE Report No. 20102*, Dept. of Geomatics Engineering, University of Calgary, Calgary, Alberta.

LI, Y.C. AND SIDERIS, M.G. (1994): Minimization and estimation of geoid undulation errors. *Bulletin Geodesique*, **68**, pp. 201-219.

PAWLOWSKI, R.S. AND HANSEN, R.O. (1990): Gravity anomaly separation by Wiener filtering. *Geophysics*, **55**(5), pp. 539-548.

SANSO, F. (1980): The minimum mean square estimation error principle in physical geodesy (stochastic and non-stochastic interpretation). *Bollettino di Geodesia e Scienze Affini*, **39**(2), pp. 112-129.

SANSO, F. AND SIDERIS, M.G. (1997): On the similarities and differences between systems theory and least-squares collocation in physical geodesy. *Bollettino di Geodesia e Scienze Affini*, **54**(2), pp. 173-206.

SCHWARZ, K.P., SIDERIS, M.G., FORSBERG, R. (1990): The use of FFT techniques in physical geodesy. *Geophysical Journal International*, **100**, pp. 485-514.

SIDERIS, M.G. (1996): On the use of heterogeneous noisy data in spectral gravity field modelling methods. *Journal of Geodesy*, **70**(8), pp. 470-479.

TZIAVOS, I.N., SIDERIS, M.G., LI, J. (1996): Optimal spectral combination of satellite altimetry and marine gravity data. *Finnish Geodetic Institute Report*, **96**(2), pp. 41-56.

TZIAVOS, I.N., FORSBERG, R., SIDERIS, M.G. (1998): Marine gravity field modelling using shipborne gravity and geodetic mission altimetry data. *Geomatics Research Australasia*, **69**, pp. 1-18.

UNSER, M. (2000): Sampling – 50 years after Shannon. *IEEE Proceedings*, **88**(4), pp. 569-587.

VASSILIOU, A.A. (1986): Numerical techniques for processing airborne gradiometer data. *UCGE Report No. 20017*, Dept. of Geomatics Engineering, University of Calgary, Calgary, Alberta.

WU, L. AND SIDERIS, M.G. (1995): Using multiple-input single-output system relationships in post processing of airborne gravity vector data. In: Schwarz, K.P. (ed.) “Airborne Gravimetry”, Proceedings of the IAG Symposium on Airborne Gravity Field Determination, IUGG XXI General Assembly, Boulder, Colorado, July 2-14, pp. 87-94.